

FEDSM-ICNMM2010-1000,

## EFFECT OF CHORDWISE FLEXIBILITY AND DEPTH OF SUBMERGENCE ON AN OSCILLATING PLATE UNDERWATER PROPULSION SYSTEM

**Oleksandr Barannyk\***  
Email: barannyk@uvic.ca

**Brad Buckham**  
Email: bbuckham@uvic.ca

**Peter Oshkai**  
Email: poshkai@uvic.ca

Institute of Integrated Energy Systems  
Department of Mechanical Engineering  
University of Victoria  
Victoria, B.C. V8W 3P6

### ABSTRACT

*This work was dedicated to the experimental study of oscillating plate propulsors undergoing a combination of heave translation and pitch rotation. The oscillation kinematics are inspired by swimming mechanisms employed by fish and other marine animals. The primary focus was on the propulsive characteristics of such oscillating plates, which were studied by means of direct force measurements in the thrust-producing regime. Experiments were performed at constant Reynolds number and constant heave amplitude. By varying the Strouhal number, the depth of submergence and the chordwise flexibility of the plate, it was possible to investigate corresponding changes in the generated thrust and the hydromechanical efficiency. It was possible to establish a set of parameters, including the driving frequency of the system, the ratio of rigid to flexible segment length of the plate, and the range of Strouhal numbers that led to a peak efficiency of approximately 80%. The experiments involving plates with various ratios of rigid to flexible segment lengths showed that greater flexibility increased the propulsive efficiency and thrust compared to an identical motion of the purely rigid plate. By submerging the plate at different depths, it was observed that the proximity of the propulsor to the bottom of the channel led to overall increase in the thrust coefficient.*

### INTRODUCTION

For centuries, aquatic species have developed highly efficient swimming mechanics that are individually optimized to their specific natural habitat. Inspired by observations of fish and marine mammals, scientists and engineers have invented vehicles whose operating principles attempt to mimic swimming kinematics. The ability of various species to achieve high velocities, rapidly change direction or to hover at a spot in moving water, are very desirable for autonomous underwater vehicles (AUVs). AUV applications in security, science and remote monitoring require the high efficiency, stability and manoeuvrability believed possible if biomimetic propulsion can be employed.

It is common knowledge that fish achieve propulsion by using their muscles to oscillate their tails. However, some muscles are not directly responsible for the gross tail locomotion, but rather to modulate the effective stiffness of the tail. This was shown by Long [1], after series of experiments on a largemouth bass. These muscles actively change the mechanical property of the fish's tail in response to the changes in the regime of operation (i.e. cruising speed) or changes in the surrounding environment (i.e. current magnitude or direction).

The interest in flapping-wing, or oscillating foil devices from an engineering point of view is due to their performance and energy and material efficiencies. For aquatic vehicles, these type

---

\*Address all correspondence to this author.

of propulsors are more ecologically friendly than common propeller type propulsors [2]. Aquatic apparatus that are used for underwater exploration, accident investigations and biological data gathering, often operate in sensitive areas with considerable biodiversity, and it is important to avoid significant alteration of the local habitat. Due to the fact that an oscillating foil system operates at relatively low frequency, marine vessels equipped with these propulsors are not dangerous to surrounding aquatic life, be that fish, animals or coral reefs.

Another benefit of oscillating foil propulsors is that they are capable of operating in different regimes of motion. By employing steady periodic swimming, characterized by cyclic repetition of propulsive movements, it is possible to cover relatively large distances at a relatively constant speed [3]. On the other hand, oscillating foil propulsors are also capable of transient movements that include acceleration, escape maneuvers and sharp turns – very rapid types of motion. Finally, oscillating foils used in combination with a control device and a stabilizer can accomplish station keeping, or hovering, in the presence of significant hydrodynamic disturbances. This is especially appealing for military or scientific underwater research applications that require extended observations at one location in the ocean.

### **Force Measurement For Oscillating Foil Propulsion**

Regardless of the application, the characterization of the lift and drag forces acting on an oscillating foil is vital to the design of an oscillating foil system. Force measurement techniques used in flapping-wing propulsion experiments can be classified into direct experimental force measurement and force measurements by vorticity fields.

Sunada in [4] studied unsteady fluid dynamic forces acting on a two-dimensional wing in sinusoidal heaving and pitching motion. In that work, unsteady fluid dynamic forces were measured directly by a load cell. By using the measured fluid dynamic forces, authors identified combinations of plunging and pitching motions for maximum time-averaged thrust and for maximum efficiency.

Another example of a direct force measurement technique is presented in the work by Read et al. [5], where the experimental study of the propulsion is performed on a heaving and pitching hydrofoil, with measurement of lift and thrust forces. The article presents conditions of high performance under significant thrust production and a series of tests on a flapping foil that produced forces needed for maneuvering of an apparatus equipped with such form of propulsor.

### **The Effect Of Chordwise Flexibility And Depth Of Submergence**

There are several theoretical and experimental investigations of elasticity effects on flapping-wing propulsor. Katz in [6] found that increasing the flexibility of a foil undergoing large amplitude oscillatory motion increased the propulsive efficiency by 20%.

However, compared to a similar motion of a rigid foil, a small decrease in overall thrust was observed. These conclusions were made based on uniform chordwise flexibility and mass distribution.

One of the classical ways to increase foil's aerodynamic performance is to modify its camber [7]. An efficient camber results in a foil with very little drag, requiring less thrust to achieve lift. However, because during symmetric pitching-up flapping the windward and leeward surfaces alternate in each stroke, the fixed camber will change sign in upstroke and downstroke, and the camber will not be useful. But for pitching-down flapping, the order of the windward and leeward surfaces does not change and the camber may be useful to improve the aerodynamic characteristics [8].

Young in [9] analyzed the influence of locust wing elastic deformation on its aerodynamic characteristics. A three-dimensional computational fluid dynamics (CFD) simulation based on wing kinematics was used for that purpose. The results were validated against smoke visualizations and digital particle image velocimetry completed for real locusts. It was shown that wing deformation in locusts is important both in enhancing the efficiency of momentum transfer to the wake and in directing the aerodynamic force vector appropriately for flight.

Tatsuro in [10], [11] investigated the propulsion of a partially elastic foil and concluded that such a foil can achieve higher efficiency for a given thrust than a rigid one, and that the chordwise mass distribution and stiffness characteristics have a significant effect upon the propulsive characteristics. These conclusions were made by applying a linear theory for the foil elasticity.

The effect of surface proximity on the performance of an oscillating foil propulsor was studied in the theoretical work of [12]. It was found that the energy wasted to generated surface waves is a dominant part of efficiency drop, and that increasing submergence leads to an increase in thrust. Similar observations were reported in [13]. It was noticed that the influence of free surface waves is different for foils of different aspect ratios. A foil with a small aspect ratio generate larger free surface effects than those created by a foil with a larger aspect ratio. Henceforth, the reduction of thrust and efficiency due to induced drag is much stronger for foils with small aspect ratios.

### **Objectives**

The main goal of this research is to establish the range of parameters for the optimal performance of an oscillating flexible plate propulsion system. This propulsion system represents the caudal area of the fish linked to a caudal fin, as shown in Fig. 1, and a study of each of these parts is required.

The caudal fin can be approximated by an oscillating flexible plate, hence, this work is aimed at establishing the sensitivity of an oscillating flexible plate's propulsive performance to the chordwise flexibility and depth of submergence. This goal will be achieved through a series of experiments that involve direct

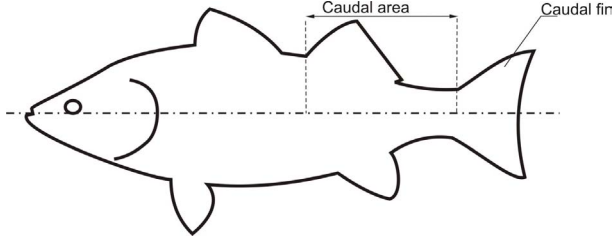


**FIGURE 1.** MAJOR PARTS OF BODY AND/OR CAUDAL FIN (BCF) LOCOMOTION.

force measurements on a plate of several rigidity types, operating in different experimental depths. The contributions of this work can be listed as follows.

- (1) Characterize the effect of chordwise flexibility of the oscillating plate on the generated thrust and efficiency through the direct force measurements on a periodically oscillating plate.
- (2) Determination of the sensitivity of the oscillating propulsion system to variation in the system driving frequency, heave amplitude and plate geometry. Identification of the set of parameters for optimal propulsive performance.
- (3) Investigation of the dependence of the propulsive characteristics of the plate on proximity to a free surface.

## EXPERIMENTAL SYSTEM AND TECHNIQUE

### Flow facility

Experiments were conducted in a flow visualization water tunnel in the Fluid Mechanics Laboratory of the Department of Mechanical Engineering at the University of Victoria. The water tunnel, schematically shown in Fig. 3, that was employed in the current investigation was of a re-circulating type, with the closed flow loop arranged in a vertical configuration. The components of the tunnel included a test section, filtering station and a circulating pump with a variable speed drive assembly. The water tunnel had a test section with 2.5m of working length, and 45cm of width and depth.

### Experimental apparatus

The present study focused on the hydrodynamics of an oscillating propulsor. A simplified geometry that involved a flat rectangular plate with blunt leading and trailing edges was considered. The plate was undergoing sinusoidal oscillatory motion with parameters that are specified in Table 1.

Three types of rectangular plate with a rigid upstream section and a flexible downstream section, as shown in Figures 2, with different ratios of rigid-to-flexible parts (1 : 0 - 100% rigid, 1 : 1 - 50%-rigid, 1 : 6 - 15%-rigid) were used to investigate the effect of chordwise flexibility on thrust coefficient  $C_T$  and efficiency  $\eta$ . All plate configurations had a span of 10cm, a chord length of 20cm, and a thickness of 1.6cm.

**TABLE 1.** PARAMETERS USED FOR EXPERIMENTS ON THE EFFECT FREE SURFACE ON PROPULSION CHARACTERISTICS OF OSCILLATING-FOIL SYSTEM.

Case	a (m)	b (m)	r (m)	f (m)	h (m)	d (m)	U (m/s)
A	0.1	0.2	0.03	0.17	0.00	0.45	0.22
B	0.1	0.2	0.03	0.17	0.08	0.45	0.22
C	0.1	0.2	0.03	0.17	0.17	0.45	0.22
D	0.1	0.2	0.03	0.17	0.25	0.45	0.22
E	0.1	0.2	0.03	0.17	0.33	0.45	0.22

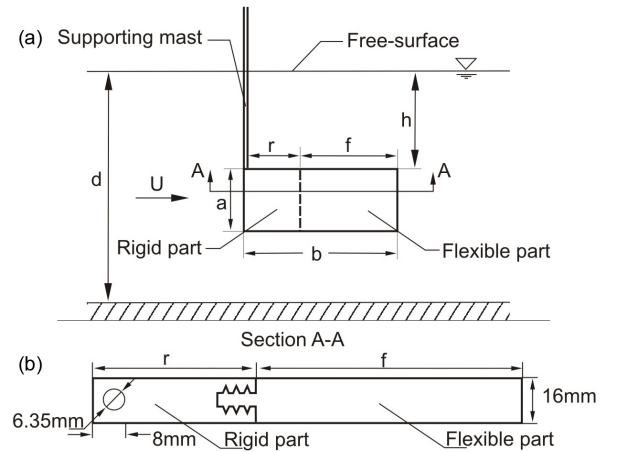


**FIGURE 2.** (a) DEFINITION OF PRINCIPAL DIMENSIONS FOR OSCILLATING PLATE (B) SECTION A-A OF THE OSCILLATING PLATE WITH CHORDWISE FLEXIBILITY

The plate was attached to an aluminium shaft, which in turn was connected to a 3-axial load cell. The 100% rigid plate and rigid parts for the plate with variable flexibility were made of acrylic. The flexible part was subsequently made of Polydimethylsiloxane (PDMS) using a molding process.

### Motion parameters and control

In the present experiments, a rectangular plate with chord length  $b$  was undergoing a combination of heave and pitch motions ( $h(t)$  and  $\theta(t)$ , respectively [14]), defined by Eqns. (1) and (2).

$$h(t) = h_0 \sin(\omega t), \quad (1)$$

$$\theta(t) = \theta_0 \sin(\omega t + \varphi). \quad (2)$$

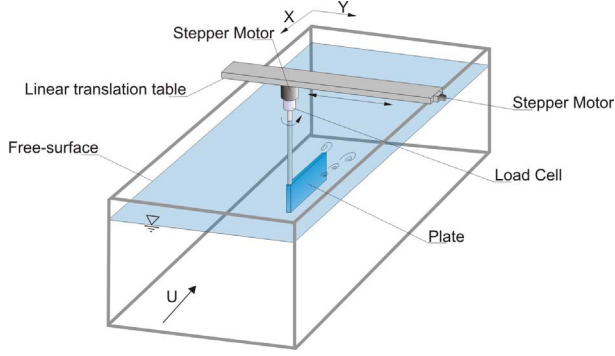


FIGURE 3. SCHEMATICS OF THE EXPERIMENTAL SETUP.

Here  $\varphi$  is the phase angle difference between pitch and heave motions,  $\omega$  is the frequency of oscillation,  $h_0$  is the amplitude of the heave motion, and  $\theta_0$  is the amplitude of pitch motion.

The choice of sinusoidal profile is based on analysis of underwater films of J. Cousteau, that were obtained in the natural habitat [2]. It was concluded that during uniform translatory motion, the trajectories of the stem and fin of a swimming dolphin are close to sine curve. It was also concluded by the authors that the pitch oscillations are lagging behind the heave oscillations by an angle close to  $\varphi = \pi/2$  which is referred as a phase angle.

The oscillating plate driving device, shown in Fig. 3, was designed to be actuated linking heave direction motion with pitch direction motion by mounting the pitch direction driving device on the heave direction drive. A 2-axis motion control and positioning system is consisted of two *Parker HV23* stepper motors, and a linear table. Motors had a resolution of 25000 steps per revolution with an error 3 – 5% per step which was non-cumulative from one step to another.

One stepper motor provided the heave motion through the Parker's *HD* series linear table with the maximum travel distance of 1000mm and the accuracy of 60 $\mu$ m. Another motor connected to PEN-023-009-S7 Parker's Precision Gearhead with 9:1 gear ratio induced the pitch motion. Both motors were operated through 6K Series Controllers, and the motion profile was programmed using native 6K programming language.

Table 1 shows the values of the experimental parameters used in the present investigation, including the length of the rigid section of the plate  $r$ , the length of the flexible section  $f$ , the plate's width  $a$ , length  $b$ , the water depth  $d$ , the distance from the plate's top edge to free surface  $h$ , and the inflow velocity  $U$ .

### Unsteady force measurements

To perform direct force measurements on the oscillating plate, a Novatech F233-Z3712 3-axial load cell was directly connected to a digital data acquisition board, which had a resolution of 16 bits per channel. The acquisition frequency was set to 400Hz; this number was chosen based on expected operational frequencies of the system and in order to satisfy the sampling

theorem [15]. Each experiment was recorded for 2 minutes, which yielded 48000 points. The duration of the experimental run made it possible to obtain from 20 to 72 full periods. A Lab-View code, virtual instrument(vi), was developed to allow simultaneous recording of unsteady force signals from all three axes of the load cell as well as heave and pitch coordinates from the motion control and positioning system.

In order to minimize the effects of electronic interference on the recorded force signals, a high-pass 3rd order filter with cut-off frequency of 0.2Hz and Chebyshev topology along with low-pass 10th order Butterworth filter with cut-off 10Hz were implemented in the Labview code and applied on the fly. In addition to that, a simple smoothing routine was written in Matlab and applied to the obtained data. Smoothing techniques are known to be efficient to reduce noise during data analysis in fields such as image processing, Doppler velocimetry, bridge monitoring or medical applications [16]. Finally, the raw force data was post-processed in Matlab by averaging every 20 data points.

## PERFORMANCE OF THE OSCILLATING PLATE PROPULSOR

### Background

When a plate undergoes an oscillatory motion in the fluid according to the parameters defined in Eqns. (1) and (2), it experiences forces  $F_x(t)$ ,  $F_y(t)$  in the  $x$ - (streamwise) and  $y$ - (transverse) directions, respectively; and torque  $M_z(t)$ . If  $T$  is the period of the oscillatory motion, the time-averaged value of  $F_x(t)$ ,  $\bar{F}_x$ , and the average input power per cycle  $\bar{P}$  are given by

$$\bar{F}_x = \frac{1}{nT} \int_0^{nT} F_x(t) dt, \quad (3)$$

$$\bar{P} = \frac{1}{nT} \left( \int_0^{nT} F_y(t) \frac{dh}{dt}(t) dt + \int_0^{nT} M_z(t) \frac{d\theta}{dt}(t) dt \right), \quad (4)$$

where  $n$  is a number of oscillation periods per run from 10 at  $St = 0.10$  to 46 at  $St = 0.46$ . The force data were used to calculate thrust and power coefficients using the following equations [14]:

$$C_T = \frac{\bar{F}_x}{\frac{1}{2} \rho ab U^2} \quad (5)$$

$$C_P = \frac{\bar{P}}{\frac{1}{2} \rho ab U^3}, \quad (6)$$

where  $b$  and  $a$  are the chord and the span of the plate, respectively, and  $\rho$  is the density of the fluid.

The propulsive efficiency is defined as a ratio of the useful

power to the input power, and is given by

$$\eta_P = \frac{\bar{F}_x U}{\bar{P}} = C_T / C_P. \quad (7)$$

One of the most important parameters related to the oscillatory plate motion is the Strouhal number based on the heave amplitude. The Strouhal number is defined as follows

$$St = \frac{fA}{U}, \quad (8)$$

where  $f$  denotes the frequency of plate oscillation in Hz (tailbeat frequency of the fish), that is  $f = \omega / (2\pi)$ , and  $A$  is a characteristic width of the created jet flow, which will be discussed later in this section. The width of the created jet flow was not known a priori and, following [17], was taken to be equal to the double of the heave amplitude, i.e.  $A = 2h_0$ .

In the present investigation, the incoming velocity  $U$  was set to  $0.22 \text{ m/s}$ , resulting in a Reynolds number  $Re = Uc/\nu$  of 44000, which is close the Reynolds number  $Re = 45000$  estimated for a striped mullet [17]. The amplitude of the heave motion  $h_0$  was set to  $0.08 \text{ m}$  and the amplitude of the pitch motion  $\theta_0$  was set to  $8^\circ$ . Moreover, this investigation was limited to a phase difference  $\varphi$  between the heaving and pitching motions equal to  $90^\circ$ , which corresponds to the optimum propulsion as reported in previous experimental studies [14], [5], [18]. Therefore, the parametric study involved variation of the oscillating frequency  $f$  in order to obtain the necessary range of Strouhal number  $St$ , which varied in our case between 0.10 and 0.46, with an increment of  $\Delta St = 0.02$ .

### Effect of chordwise flexibility of the oscillating plate

**Thrust coefficient** In Fig. 4, one can see the overall result of experimentally obtained values of thrust coefficient  $C_T$  as a function of the Strouhal number,  $St = fA/U$ . The data corresponds to the depth of submergence  $h_0 = 0.8 \text{ cm}$  (defined in Fig. 2).

It can be seen on the graph of the thrust coefficient  $C_T$ , that its value increases uniformly with the Strouhal number  $St$ . This observation coincides with the results obtained in the similar experiments by [19], [17] and [20]. As the frequency of oscillation increases, the system reaches a critical point where the oscillating plate begins to generate thrust, which corresponds to the value of the Strouhal number of  $St \approx 0.25$ . This phenomenon corresponds to the following structure of the wake generated by the plate. At the critical value of the Strouhal number, an alternating vortex pattern is formed such that the vortex with a positive (counter-clockwise) circulation is shed at the top position and the vortex with the negative (clockwise) circulation is shed at the bottom position in terms of the heave trajectory [21].

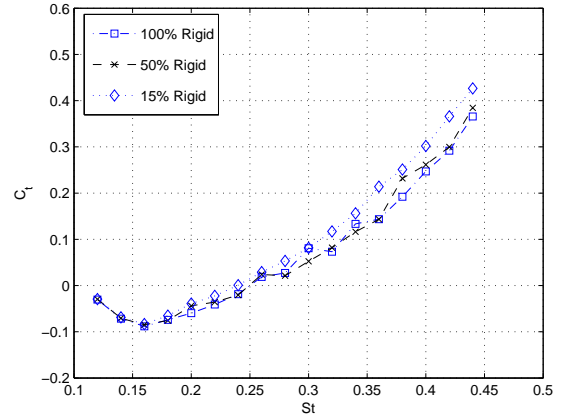


**FIGURE 4.** EXPERIMENTALLY MEASURED THRUST COEFFICIENT  $C_T$  AS A FUNCTIONS OF STROUHAL NUMBER  $St$  FOR THREE TYPES OF FLEXIBLE PLATES, 1 : 0 RATIO:  $h = 17 \text{ cm}$ ,  $r = 20 \text{ cm}$ ,  $f = 10 \text{ cm}$ ,  $\alpha_{\max} = 8^\circ$ ,  $h_0 = 8 \text{ cm}$ ,  $\varphi = 90^\circ$ ; 1 : 1 RATIO:  $h = 17 \text{ cm}$ ,  $r = 10 \text{ cm}$ ,  $f = 0 \text{ cm}$ ,  $\alpha_{\max} = 8^\circ$ ,  $h_0 = 8 \text{ cm}$ ,  $\varphi = 90^\circ$ ; 1 : 6 RATIO:  $h = 17 \text{ cm}$ ,  $r = 3 \text{ cm}$ ,  $f = 17 \text{ cm}$ ,  $\alpha_{\max} = 8^\circ$ ,  $h_0 = 8 \text{ cm}$ ,  $\varphi = 90^\circ$ .

This structure is an inverse of the well known von Kármán vortex street, that can be observed in wakes, and corresponds to the formation of an average velocity profile in the form of a jet. Hence the critical value of Strouhal number  $St$  correspond to the transformation of the wake of the oscillating propulsor from a regime corresponding to a net momentum deficit to the regime corresponding to a net momentum excess, thus producing thrust.

It can be noted that the critical value of the thrust coefficient was not the same for all three plates. The most flexible plate with 1 : 6 rigid-to-flexible ratio started to produce thrust at a slightly lower value of the Strouhal number ( $St \approx 0.24$ ) than the two other plates. This critical value depends not only on the chordwise flexibility of the plate, but also on the ratio of the heave amplitude  $h_0$  to the chord length  $b$ , and on the value of the maximum angle of attack  $\alpha_{\max}$ , as was shown in [5]. According to [5], zero crossing of the thrust coefficient  $C_T$  can vary from a very low Strouhal number ( $St = 0.10$ ) for  $h_0/c = 1.0$  and  $\alpha_{\max} = 10 - 15^\circ$  to a rather moderate value of  $St = 0.32$  for  $h_0/c = 0.75$  and  $\alpha_{\max} = 50^\circ$ . From Fig. 4 it is clear that the most flexible plate with 1 : 6 rigid-to-flexible ratio provided more thrust than the plates with 1 : 1 and 1 : 0 rigid-to-flexible part lengths ratios in propulsion regime. The propulsion regime corresponds to the range of Strouhal number  $St$  [0.24 – 0.44]. This range is in the good agreement with the range of [0.25 – 0.4] reported by [17].

Starting at a zero crossing on the thrust coefficient curves, the average percentage increase of thrust coefficient  $C_T$  for the plate with 1 : 1 rigid-to-flexible ratio compared to the plate with 1 : 0 rigid-to-flexible ratio was equal to 13%. For the plate with 1 : 6 rigid-to-flexible ratio compared to the plate with 1 : 0 rigid-

to-flexible ratio, the thrust coefficient increased by 27%. During the thrust-generating regime, the values of thrust coefficient  $C_T$  agreed with results reported by [13] and [22]. It can be concluded that modifying the ratio of the rigid-to-flexible part length of the oscillating plate can lead to an increase in thrust coefficient.

**Efficiency** In Fig. 5, plots of efficiency as a function of time, obtained for the same range of the motion parameters as the ones for the thrust coefficient  $C_T$ , are presented. The maximum values for the efficiency for all three cases are 48%, 34% and 27% for the plates with 1 : 6, 1 : 1 and 1 : 0 rigid-to-flexible ratios respectively. Those peaks occur in the range of the Strouhal number  $St$  [0.25 – 0.35], confirming that the maximum efficiency is achieved in the range suggested by [17].

Each curve in Fig. 5 corresponds to the efficiency evolution for one of possible three choices of plate with 1 : 6, 1 : 1 and 1 : 0 rigid-to-flexible ratios. As with the thrust coefficient  $C_T$ , the efficiency of 1 : 6 rigid-to-flexible ratio plate is higher than that of the other two plates. This can be explained if one considers the change of the plate's curvature along its path, as was proposed in [6]. It can be seen that with the increase of the curvature of the plate, caused by forced heave and pitch motions, instantaneous lift decreases, however the orientation of the resulting lift is nearer the direction of advance, which in turn suggests higher efficiency.

However, the high efficiency peaks that were obtained, correspond to relatively low value of thrust coefficient  $C_T$ , (less than 0.1) for all three cases and hence have limited relevance for propulsion applications. Similar results were reported by [5], where maximum efficiency of 75% was found. However, this value was achieved at the value of the Strouhal number for which the thrust coefficient was equal to 0.16. In the range of  $St$  corresponding to the high  $C_T$ , the efficiency of the oscillating propulsor was found to be approximately 55% [5].

The difference between the results reported in [5] and those of the present investigation is most importantly due to the geometry of the plate. Sharp corners at the leading edge of the plate produce flow separation, which in turns results in strong reduction of the suction force component leading to the rapid decrease in efficiency. The importance of avoiding such scenario, when flapping foil propulsion is greatly influenced by leading edge flow separation, was first pointed out in [23]. Intensive numerical study of the effects of dynamic stall on propulsive efficiency in [24] converged to the same conclusion. The authors reported a rapid decrease in efficiency when the leading edge flow separation was observed. However leading edge flow separation does not always cause a rapid drop in the efficiency. Anderson in [14] showed experimentally that under the right parameter values there is a constructive interaction of the leading and trailing edge vortices, which in turn improves the propulsive performance.

Other differences between the current results and those reported in [5] are mainly due to the type of propulsor used and

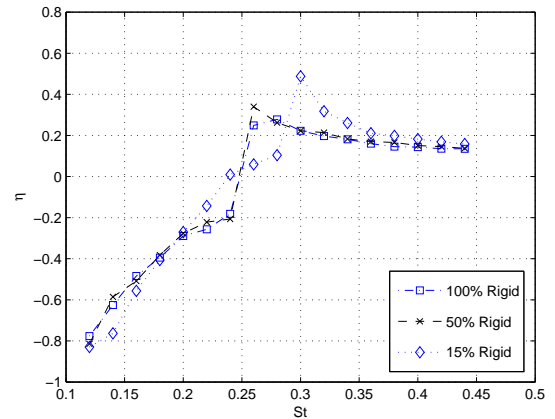


**FIGURE 5.** EXPERIMENTALLY MEASURED EFFICIENCY  $\eta$  AS A FUNCTIONS OF STROUHAL NUMBER  $St$  FOR THREE TYPES OF FLEXIBLE PLATES, 1 : 0 RATIO:  $h = 17\text{cm}$ ,  $r = 20\text{cm}$ ,  $f = 10\text{cm}$ ,  $\alpha_{\max} = 8^\circ$ ,  $h_0 = 8\text{cm}$ ,  $\varphi = 90^\circ$ ; 1 : 1 RATIO:  $h = 17\text{cm}$ ,  $r = 10\text{cm}$ ,  $f = 0\text{cm}$ ,  $\alpha_{\max} = 8^\circ$ ,  $h_0 = 8\text{cm}$ ,  $\varphi = 90^\circ$ ; 1 : 6 RATIO:  $h = 17\text{cm}$ ,  $r = 3\text{cm}$ ,  $f = 17\text{cm}$ ,  $\alpha_{\max} = 8^\circ$ ,  $h_0 = 8\text{cm}$ ,  $\varphi = 90^\circ$ .

different amplitude to chord ratios. The latter parameter in particular, as indicated by [6] and experimentally verified by [5] and [18] has significant impact on thrust coefficient  $C_T$  and efficiency  $\eta$ . Ideally, for a propulsion system one requires high efficiency in conjunction with high thrust, and in Fig. 5 one can see that efficiency tangentially approaches a value of  $\approx 18\%$  in the range of Strouhal number  $St$  [0.35 – 0.40]. This interval corresponds to higher values of thrust coefficient  $C_T$  and hence is more applicable.

Yamamoto et al. in [22] performed similar experiments on a ship model equipped with harmonically oscillating propulsion mechanism. The authors tested fins of different chordwise flexibility and showed that the fin with 1 : 6 rigid-to-flexible ratio, achieved the better overall efficiency of 31% then the other 6 prototypes reported in the article. Comparing the results obtained in [22] with those reported here, it can be seen that the most flexible plate with 1 : 6 rigid-to-flexible ratio also performed better than the other two. It was possible to achieve as much as 48% efficiency for the plate with 1 : 6 rigid-to-flexible ratio. Hence it can be concluded that increase in chordwise flexibility leads to the increase in propulsive efficiency.

### Effect of heave amplitude

The next step was to consider fixed values of the forcing frequency corresponding to the peak values of Strouhal number on the efficiency curves for each of the plates and vary the heave amplitude in such a way that the Strouhal varies in the range of  $St \in [0.10, 0.44]$ . This approach, combined with the experiments that involved variation of the oscillation frequency at a fixed value of heave amplitude, provides additional insight into

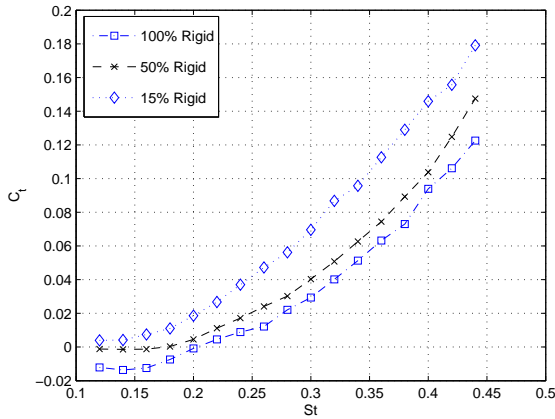


**FIGURE 6.** EXPERIMENTALLY MEASURED THRUST COEFFICIENT  $C_T$  AS A FUNCTIONS OF STROUHAL NUMBER  $St$  FOR THREE TYPES OF FLEXIBLE PLATES, 1 : 0 RATIO:  $h = 17cm$ ,  $r = 20cm$ ,  $f = 10cm$ ,  $\alpha_{max} = 8^\circ$ ,  $h_0 \in [6.4cm, 23.6cm]$ ,  $\phi = 90^\circ$ ; 1 : 1 RATIO:  $h = 17cm$ ,  $r = 10cm$ ,  $f = 0cm$ ,  $\alpha_{max} = 8^\circ$ ,  $h_0 \in [7.3cm, 26.9cm]$ ,  $\phi = 90^\circ$ ; 1 : 6 RATIO:  $h = 17cm$ ,  $r = 3cm$ ,  $f = 17cm$ ,  $\alpha_{max} = 8^\circ$ ,  $h_0 \in [6.8cm, 24.8cm]$ ,  $\phi = 90^\circ$ .

performance of an oscillating plate as a propulsor. The maximum values of the efficiency for all three cases are presented in Fig. 5. They are 48% (at  $St = 0.3$ ), 34% (at  $St = 0.26$ ) and 27% (at  $St = 0.28$ ) for 1 : 6, 1 : 1 and 1 : 0 rigid-to-flexible ratio plates respectively. For these values of Strouhal number, the corresponding values of heave oscillating frequencies are 0.41Hz, 0.36Hz and 0.29Hz for 1 : 6, 1 : 1 and 1 : 0 rigid-to-flexible ratio plates.

The peak-to-peak amplitude of plate oscillation was varying in the range of  $h_0 = [64mm - 236mm]$  for 1 : 6 rigid-to-flexible ratio plate,  $[73mm - 269mm]$  for 1 : 1 rigid-to-flexible ratio plate and  $[68mm - 248mm]$  for 1 : 0 rigid-to-flexible ratio plate. The plots of thrust coefficient and efficiency are presented in Fig. 6 and Fig. 7, respectively.

**Thrust coefficient** From the graph of the thrust coefficient  $C_T$ , one can see that the general dynamics in the behavior is similar to the results presented in Fig. 4, thrust increases almost linearly starting from  $St = 0.17$ . However, on this graph, it was possible to capture more details on differences between the performances of the three plates. It can be seen that for the lowest value of the Strouhal number the most flexible plate, with 1 : 6 rigid-to-flexible ratio, starts producing positive thrust from the very beginning.

The next plate under consideration is the one with 1 : 1 rigid-to-flexible ratio. It can be observed that, for the smallest value of the amplitude, the generated thrust was equal to zero. However, with the increase of oscillating amplitude on the heave axis, one can see that plate started to produce positive thrust at  $St = 0.18$  and continues to do that through all of the data set. The plate

with 1 : 0 rigid-to-flexible ratio produced negative thrust up to the value of the Strouhal number of  $St = 0.2$ , after that with almost the same slope as in the previous two cases, it produced positive thrust. Comparing these plots, with those presented in Fig. 4, it can be concluded that spanwise flexibility does affect the thrust production in a positive way. The most flexible plate that was used in this sets of experiments produced higher thrust. In addition, with fixed optimal frequency of oscillation, the most flexible plate started to produce thrust faster than the other two plates, and at the lowest values of oscillating amplitude.

**Efficiency** Using the same range of motion parameters, the efficiency curves plotted from experimental data are presented in Fig. 7. One can see that the shape of the graphs is topologically similar to the ones presented in Fig. 5. Three distinct regimes can be observed. The regime of gradual increase of efficiency for each of the plates lasts until efficiency reaches its maximum value. The regime of maximum efficiency, the value of Strouhal number at which the efficiency is maximum, and the regime of gradual decrease where the efficiency decreases with the increase of Strouhal number and eventually asymptotically reaches the limiting value.

It can be seen that the data obtained from experiment 2, where the amplitude of oscillation was varied, was adjusted so that the range of Strouhal number is the same as in experiment 1, where the oscillating frequency was varied, gives good understanding on propulsive differences between the three plate designs. By combining graphs from experiment 1 with those corresponding to experiment 2, where the amplitude of oscillation was varying, the observation similar to one from the analysis of thrust curves can be presented. The three plates had a very different impact on efficiency performance of the propulsion system. As in the case with thrust coefficient, the most rigid plate started to operate in the negative regime. As the chordwise flexibility increased, by changing the type of the plate to the one with 1 : 1 rigid-to-flexible ratio, it can be seen that second plate initially produced zero efficiency for two values of oscillating amplitude resulted in growth of efficiency as a function of Strouhal number. However, the most flexible plate already starts at 15% efficiency value for the smallest value of heave amplitude, and continues to produce positive efficiency with the increase of the Strouhal number. It can be concluded from the graphs presented in Fig. 4 – 7 that the Strouhal number, oscillating frequency and heave amplitude triplets such as  $\{St = 0.3, f = 0.41Hz, h_0 = 16.1cm\}$ ,  $\{St = 0.26, f = 0.36Hz, h_0 = 15.9cm\}$  and  $\{St = 0.28, f = 0.29Hz, h_0 = 15.8cm\}$  for 1 : 6, 1 : 1 and 1 : 0 rigid-to-flexible ratio plates respectively, are the optimal parameter combinations that allow oscillating plate propulsion system to operate in thrust-producing regime with highest efficiency.

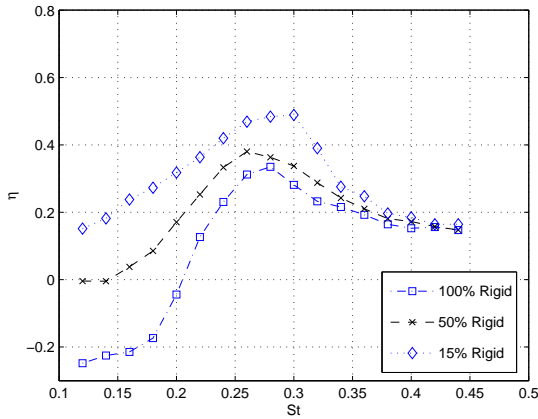


**FIGURE 7.** EXPERIMENTALLY MEASURED EFFICIENCY  $\eta$  AS A FUNCTIONS OF STROUHAL NUMBER  $St$  FOR THREE TYPES OF FLEXIBLE PLATES, 1 : 0 RATIO:  $h = 17cm, r = 20cm, f = 10cm, \alpha_{max} = 8^\circ, h_0 \in [6.4cm, 23.6cm], \phi = 90^\circ$ ; 1 : 1 RATIO:  $h = 17cm, r = 10cm, f = 0cm, \alpha_{max} = 8^\circ, h_0 \in [7.3cm, 26.9cm], \phi = 90^\circ$ ; 1 : 6 RATIO:  $h = 17cm, r = 3cm, f = 17cm, \alpha_{max} = 8^\circ, h_0 \in [6.8cm, 24.8cm], \phi = 90^\circ$ .

### Depth of submergence

When the plate is oscillating in an unbounded fluid, the horizontal thrust is equals to the mean momentum transport in the wake, which is formed behind the plate. From this observation it follows that the wasted energy is mainly due to the wake formation. When a free surface is present, the problem becomes much more complicated, because the waves always give rise to a considerable amount of wasted energy. The plate in close proximity to a free surface will generate surface waves that may transport large amount of momentum downstream. Depending on the properties of generated waves, this momentum transport might be either positive or negative. This momentum transport, in turn, will lead to an increase or decrease in thrust and efficiency.

In order to investigate the effect of the free surface on propulsion characteristics of the oscillating-plate, experiments were performed at five depths of submergence, specified in Table 1.

**Thrust coefficient** In Fig. 8, detailed experimental investigation of the propulsive characteristics of an oscillating plate for different experimental depths is presented. Only the most flexible plate with 1 : 6 rigid-to-flexible ratio was used in the current experiment, because it displayed the highest efficiency in other tests involving  $St$  variation. Range of parameters used in experiments is presented in Table 1. Comparison of the measured thrust coefficient  $C_T$  near bottom of the channel (Case E) in middepth (Case C) and near free surface (Case A) and in intermediate cases showed that the plate oscillating near channel floor has a larger thrust over almost the entire considered range

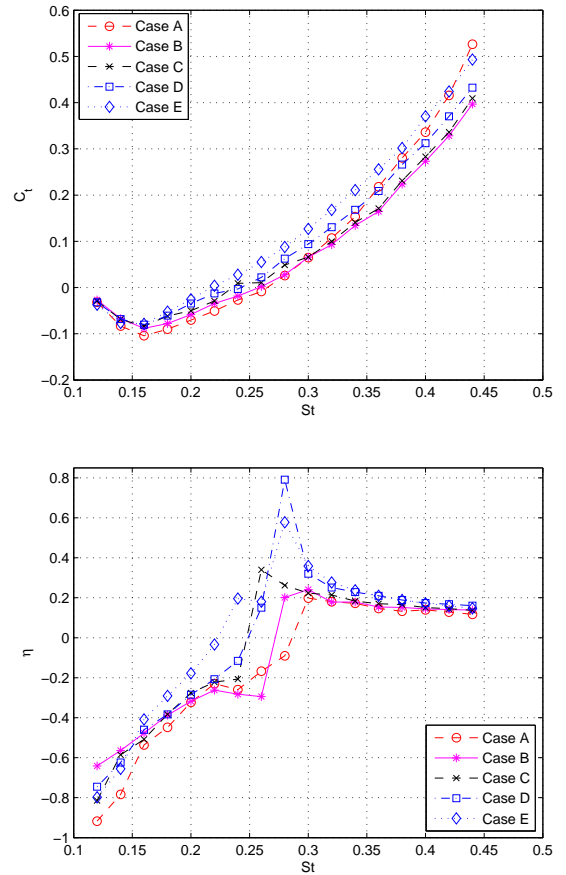


**FIGURE 8.** EXPERIMENTALLY MEASURED THRUST COEFFICIENT AND EFFICIENCY AS A FUNCTION OF STROUHAL NUMBER  $St$  for 1 : 6-RATIO PLATE. CASE A:  $h = 0cm, r = 3cm, f = 17cm, \alpha_{max} = 8^\circ, h_0 = 8cm, \phi = 90^\circ$ ; CASE B:  $h = 8cm, r = 3cm, f = 17cm, \alpha_{max} = 8^\circ, h_0 = 8cm, \phi = 90^\circ$ ; CASE C:  $h = 17cm, r = 3cm, f = 17cm, \alpha_{max} = 8^\circ, h_0 = 8cm, \phi = 90^\circ$ ; CASE D:  $h = 25cm, r = 3cm, f = 17cm, \alpha_{max} = 8^\circ, h_0 = 8cm, \phi = 90^\circ$ ; CASE E:  $h = 33cm, r = 3cm, f = 17cm, \alpha_{max} = 8^\circ, h_0 = 8cm, \phi = 90^\circ$ .

of Strouhal number. It was found that operating the plate near water surface (Case B) changed the thrust only slightly from the value produced at middepth (Case C).

Due to the position of the plate, i.e. in a vertical plane, the dependance of the thrust coefficient on the depth of submergence is limited, because only the upper part of the plate interacts with free surface while most of the plate stayed submerged. However, since the span length in our case was not very large the surface patterns still affected propulsive characteristics of the plate, even though not as strongly as for the horizontally submerged plate(not considered herein).

These results confirm theoretical study done by Grue et al. in [12]. The authors found that the energy waste due to gener-

ated surface waves is a dominant part of the waste and increasing of submergence depths leads to the increase in thrust. Similar observations were reported in [13]. The authors noticed that influence of the foil generated free surface waves is different for the foils of different aspect ratios. The foil with small aspect ratio generates larger free surface effects than those created by a foil with larger aspect ratio. Thus, the reduction of thrust and efficiency due to induced drag is more pronounced for the foil with small aspect ratio.

When the plate was positioned tangent to the free surface, the variation in the thrust coefficient  $C_T$  was different from that for all cases considered earlier. One can see that starting at  $St \approx 0.30$  there is a steep rise in thrust coefficient, whilst the efficiency asymptotically approaches its limit. It is possible to highlight two physical mechanisms behind this phenomenon. When the plate undergoes periodic oscillations, part of the waves generated propagates in the same direction as the plate's translation, these will induce drag on the plate. However, there will be waves that propagate in the opposite direction which will generate thrust. Hence, the magnitude of those propagating waves will affect the overall thrust. Another possibility lies in the interaction between free surface waves and vorticity in the wake. It is possible that for the range of the Strouhal number,  $St = [0.30 - 0.45]$ , the energy of the bow wave, created by the leading edge of the plate, is absorbed by the trailing edge in the process of wake generation which will lead to increase in thrust. In order to provide the definite answer regarding the mechanism of this phenomenon, further investigations are required.

**Efficiency** Plots of the efficiency for various submerging depths are shown in Fig. 8. Here, the plate with 1 : 6 rigid-to-flexible ratio is presented. Similarly to the results for the thrust coefficient  $C_T$ , the overall improvement of the efficiency  $\eta$  with the increase of submergence depth was observed. Comparing plots for different experimental depths, it can be seen that cases A, and B for the range of the Strouhal number  $St = [0.10 - 0.22]$ , where both thrust and efficiency are negative, and  $St = [0.30 - 0.45]$  which corresponded to the highest thrust, mostly coincide with each other. Case C showed substantial increase in efficiency. This phenomenon can be attributed to the change of the orientation of the generated lift force, caused by the curvature of the large area of the plate, as was proposed in [6].

Zhu in [13] noticed that the influence of foil generated free surface waves is different for foils of different aspect ratios. In cases involving small aspect ratio the reduction of thrust and efficiency due to induced drag is accompanied by much larger free surface effects than those created by foils with aspect higher ratio. Zhu reported that for large aspect ratio foil the maximum changes caused by free surface in thrust and efficiency are 3% and 11% respectively. While the effect of free surface on a small aspect ratio foil leads to reduction of 8% and 40% on thrust and

efficiency. The plate presented in current experiments has a small aspect ratio  $a/b = 0.5$ , and from the Fig. 8, a reduction of more than 44% for thrust coefficient and 66% for efficiency can be observed. It follows that small aspect ratio foils are more sensitive to the free surface effects.

Another interesting result is that the highest value of efficiency was observed near the bottom of the water channel (Case D) and (Case E). This effect can be contributed to the ground effects, similar to those experienced by high-speed ground vehicles, birds and bottom-dwelling fishes. It can be concluded that the ground effect in the present case leads to an increase in propulsive efficiency. Similar conclusion was reached by [25] in his theoretical investigation of ground effect on propulsion of birds and fishes.

The results for the propulsive characteristics of the plate with 1 : 6 rigid-to-flexible ratio were compared to the plots for the plates with 1 : 0 and 1 : 1 rigid-to-flexible ratios(not shown here). The most flexible plate produced 7% more thrust compared to the most rigid one, for identical geometric and kinematic parameters. This observation confirmed conclusions of the previous section that the thrust coefficient generally increases with the increase of chordwise flexibility of the plate.

## CONCLUSIONS

The main objectives of this work was the comparison study of the caudal fin kinematics and mechanics. The caudal fin motion was represented by an oscillating plate propulsion system.

The direct force measurements were used to confirm that a more elastic plate has better propulsion characteristics, namely thrust and efficiency, than the completely rigid one. By fixing the oscillating frequency at the values of Strouhal number that correspond to the maximum efficiency, the peak-to-peak amplitude of oscillation was varied in order to optimize the thrust and efficiency. It was concluded that Strouhal number, oscillating frequency and heave amplitude triplets such as  $\{St = 0.3, f = 0.41Hz, h_0 = 16.1cm\}$ ,  $\{St = 0.26, f = 0.36Hz, h_0 = 15.9cm\}$  and  $\{St = 0.28, f = 0.29Hz, h_0 = 15.8cm\}$  for 1 : 6, 1 : 1 and 1 : 0 rigid-to-flexible ratio plates respectively, are the optimal values that allow oscillating plate propulsion system to operate in thrust producing regime with highest efficiency.

The set of experiments for the plate oscillating at different depth of submergence showed that depth increase leads to the increase in propulsive characteristics of the plate. With respect to experimental depth, the increase in thrust coefficient and efficiency was not linear. In the region from free surface to mid-depth, the increase in the thrust coefficient was not significant. However, in the region from middepth to the floor of the test section of the water channel, the increase of the thrust coefficient was more profound. The special case when the plate was tangential to the free surface showed that, for plates of all types of chordwise flexibility, there is a steep rise in thrust coefficient as a function of the Strouhal number, while the efficiency asymptoti-

cally approaches its limit.

The high efficiency value that was observed near the channel floor is suggested to be due to the ground effects on the oscillating plate.

A rapid decrease in propulsive efficiency as a function of  $St$  after it reached its maximum was observed in all experiments. Possible ways to avoid this effect would be to change the cross section of the plate to a NACA profile and increase the aspect ratio. Visualization of the free surface effects combined with quantitative flow imaging will provide additional insight into the mechanism of interaction between free surface patterns generated by the propulsor and the shed vorticity.

## REFERENCES

- [1] Long, J. H., and Nipper, K. S., 1996. "The importance of body stiffness in undulatory propulsion". *American Zoologist*, **36**, pp. 678–694.
- [2] Rozhdestvensky, K. V., and Ryzhov, V. A., 2003. "Aerohydrodynamics of flapping-wing propulsors". *Progress in Aerospace Sciences*, **39**(8), pp. 585–633.
- [3] Sfakiotakis, M., Lane, D. M., and Davies, J., 1999. "Review of fish swimming modes for aquatic locomotion". *Ieee Journal of Oceanic Engineering*, **24**(2), pp. 237–252.
- [4] Sunada, S., Kawachi, K., Matsumoto, A., and Sakaguchi, A., 2001. "Unsteady forces on a two-dimensional wing in plunging and pitching motions". *Aiaa Journal*, **39**(7), pp. 1230–1239.
- [5] Read, D. A., Hover, F. S., and Triantafyllou, M. S., 2003. "Forces on oscillating foils for propulsion and maneuvering". *Journal of Fluids and Structures*, **17**(1), pp. 163–183.
- [6] Katz, J., and Weihs, D., 1978. "Hydrodynamic propulsion by large-amplitude oscillation of an airfoil with chordwise flexibility". *Journal of Fluid Mechanics*, **88**, pp. 485–497.
- [7] Abbott, I. H., and Doenhoff, A. E. v., 1959. *Theory of wing sections. Including a summary of airfoil data*. Dover, New-York.
- [8] Bai, P., Cui, E.-j., and Zhan, H.-l., 2009. "Aerodynamic Characteristics, Power Requirements and Camber Effects of the Pitching-Down Flapping Hovering". *Journal Of Bionic Engineering*, **6**(2), JUN, pp. 120–134.
- [9] Young, J., Walker, S. M., Bomphrey, R. J., Taylor, G. K., and Thomas, A. L. R., 2009. "Details of insect wing design and deformation enhance aerodynamic function and flight efficiency". *SCIENCE*, **325**(5947), pp. 1549–1552.
- [10] Tatsuro, K., Hiroharu, K., Akihiro, K., and Hajime, Y., 1984. "Study on propulsion by partially elastic oscillating foil (1st report). analysis by linearized theory". *Journal of the Society of Naval Architects of Japan*, **156**, pp. 82–101.
- [11] Tatsuro, K., Hiroharu, K., Akihiro, K., and Hajime, Y., 1984. "Study on propulsion by partially elastic oscillating foil (2nd report). numerical simulations by singularity distribution method and evaluation of scompe for application to ship propulsion.". *Journal of the Society of Naval Architects of Japan*, **156**, pp. 92–101.
- [12] Grue, J., Mo, A., and Palm, E., 1988. "Propulsion of a foil moving in water-waves". *Journal of Fluid Mechanics*, **186**, pp. 393–417.
- [13] Zhu, Q., Liu, Y. M., and Yue, D. K. P., 2006. "Dynamics of a three-dimensional oscillating foil near the free surface". *AIAA Journal*, **44**, pp. 2997–3009.
- [14] Anderson, J. M., Streitlien, K., Barrett, D. S., and Triantafyllou, M. S., 1998. "Oscillating foils of high propulsive efficiency". *Journal of Fluid Mechanics*, **360**, pp. 41–72.
- [15] D'antona, G., and Ferrero, A., 2006. *Digital Signal Processing for Measuring Systems. Theory and Applications*. Springer.
- [16] Levesque, L., 2008. "Simple smoothing technique to reduce data scattering in physics experiments". *European Journal of Physics*, **29**(1), pp. 155–162.
- [17] Triantafyllou, G. S., Triantafyllou, M. S., and Grosenbaugh, M. A., 1993. "Optimal thrust development in oscillating foils with application to fish propulsion". *Journal of Fluids and Structures*, **7**(2), pp. 205–224.
- [18] Schouveiler, L., Hover, F. S., and Triantafyllou, M. S., 2005. "Performance of flapping foil propulsion". *Journal of Fluids and Structures*, **20**(7), pp. 949–959.
- [19] Koochesfahani, M. M., 1989. "Vortical patterns in the wake of an oscillating airfoil". *Aiaa Journal*, **27**(9), pp. 1200–1205.
- [20] Isshiki, N., Mirikawa, H., and Kato, H., 1980. "The study on a propulsion system by fin stroke.". *Bulletin of Marine Engineering Society in Japan*, **8**(1), pp. 71–79.
- [21] Barannyk, O., 2009. *Effect of chordwise flexibility and depth of submergence on an oscillating plate underwater propulsion system*. MASC Thesis, University of Victoria.
- [22] Yamamoto, I., Terada, Y., Nagamatu, T., and Imaizumi, Y., 1995. "Propulsion system with flexible rigid oscillating fin". *IEEE Journal of Oceanic Engineering*, **20**(1), pp. 23–30.
- [23] Lighthill, J., 1970. "Aquatic animal propulsion of high hydromechanical efficiency". *Journal of Fluid Mechanics*, **44**(NOV11), p. 265.
- [24] Isogai, K., Shinmoto, Y., and Watanabe, Y., 1999. "Effects of dynamic stall on propulsive efficiency and thrust of flapping airfoil". *AIAA Journal*, **37**(10), pp. 1145–1151.
- [25] Tanida, Y., 2001. "Ground effect in flight - (birds, fishes and high-speed vehicle)". *JSME International Journal Series B-Fluids and Thermal Engineering*, **44**(4), pp. 481–486.